Advanced Materials Research Vol. 409 (2012) pp 859-864
© (2012) Trans Tech Publications, Switzerland
doi:10.4028/www.scientific.net/AMR.409.859

Determination of Global and Local Tensile Behaviours of Laser Welded Ti-6Al-4V Alloy

Abu Syed Humaun Kabir [1, 2, a], Xinjin Cao [2, b], Javad Gholipour Baradari [2, d], Priti Wanjara [2, g], Jonathan Cuddy [3, e], Anand Birur [3, f], and Mamoun Medraj [1, c]

[1]Department of Mechanical Engineering, Concordia University, 1455 De Maisonneuve Blvd. West, Montreal, Quebec, Canada, H3G 1M8
[2]Aerospace Manufacturing Technology Centre, NRC Institute for Aerospace Research, 5145 Decelles Ave., Montreal, Quebec, Canada, H3T 2B2
[3]Standard Aero Limited, 33 Allen Dyne Road, Winnipeg, Manitoba, Canada, R3H 1A1

[a] k_abusy@encs.concordia.ca, [b] xinjin.cao@cnrc-nrc.gc.ca, [c] mmedraj@encs.concordia.ca
[d] Javad.GholipourBaradari@cnrc-nrc.gc.ca, [e] Jonathan.Cuddy@StandardAero.com,
[f] Anand_birur@StandardAero.com, [g] priti.wanjara@cnrc-nrc.gc.ca

Keywords: Nd:YAG laser; Titanium alloy; Ti-6Al-4V; Tensile properties

Abstract. In this study, the global and local tensile behaviours of laser welded 5.1-mm thick Ti-6Al-4V alloy were obtained at various welding speeds and defocusing distances using a digital image correlation (DIC) technique with a full field three-dimensional deformation measurement system. The local tensile properties including elastic modulus, yield stress, and maximum plastic strain were determined at various locations by assuming an iso-stress condition. It was found that the elastic modulus and yield stress were maximum in the fusion zone (FZ) and minimum in the heat-affected zone (HAZ). Porosity and underfill defects were the main reasons for the failures in the FZ and/or the HAZ. Maximum plastic strain at fracture was observed at the failure location in most cases.

Introduction

Ti-6Al-4V is an α + β titanium alloy that contains 6 wt% Al, and 4 wt% V. Aluminum stabilizes the HCP α-phase while vanadium stabilizes the BCC β-phase at lower temperatures, and therefore Ti-6Al-4V usually comprises of these two phases at room temperature [1]. Ti-6Al-4V is one of the very first titanium alloys developed and remains by far the most popular, accounting for more than 50% usage amongst all commercial grades [2]. The high strength to weight ratio and excellent corrosion resistance of Ti-6Al-4V have led to a wide and diverse range of successful applications, particularly in the aerospace industry, where this grade accounts for more than 80% of all titanium alloy usage [3]. Though Ti-6Al-4V is limited to applications where the working temperature is less than 300°C [4], it is ranked with high weldability amongst the α + β alloys [5]. Previous work has reported that the tensile ductility of Ti-6Al-4V is directly affected by the FZ and HAZ dimensions, microstructures, grain sizes, and defects [6]. The weld ductility can be degraded by the coarse prior-β grain size due to the tendency of crack propagation along the prior-β grain boundary [7]. Laser welding produces a smaller prior-β grain size than conventional arc welding processes due to the lower heat input and higher cooling rate [7]. Cao et al. [1] showed that for 2-mm thick Ti-6Al-4V sheets, the yield and tensile strengths increase with increasing welding speed, but Mazumder and Steen [8] did not find significant differences in the global tensile properties with variations in welding speed and laser power for 1- and 2-mm thick Ti-6Al-4V. To better understand the influence of the process parameters on the mechanical properties, the heterogeneous characteristics of the weldment, namely the different structural features in the HAZ and FZ relative to the base metal (BM), need to be further studied. It is expected that each zone may have different mechanical properties. The tensile behaviours of each zone, referred to as the local tensile properties in this work, were determined and differentiated from the global (overall) tensile properties that are usually obtained from the conventional transverse tensile test data. To date, the DIC technique has been used to study the local tensile properties of friction stir welded aluminum alloys [9] and laser

All rights reserved. No part of contents of this paper may be reproduced or transmitted in any form or by any means without the written permission of TTP, www.ttp.net. (ID: 132.246.225.127-24/11/11,15:37:08)

welded stainless steel [10], but has never been applied for laser welded Ti-6Al-4V. DIC is a non-contact optical technique that is capable of measuring full-field two-dimensional (2-D) or three-dimensional (3-D) surface deformations. It is a highly responsive method with wide tolerances in sample size that requires a simple surface treatment on the test samples [11].

Experimental procedures

The material used was grade 5 Ti-6Al-4V alloy, that was received in sheet form with a thickness of 5.1 mm. The welding equipment consisted of a 4 kW continuous wave (CW) solid-state Nd: YAG laser system equipped with an ABB robot and a magnetic holding fixture. A collimation lens of 200 mm, a focal lens of 150 mm and a fiber diameter of 0.6 mm were used to produce a focal spot diameter of approximately 0.45 mm. The weld surfaces were shielded by inert gases due to the high reactivity of titanium with atmospheric elements (oxygen, nitrogen and hydrogen) at high temperature. In this study, the maximum power of the laser, 4 kW, was used. Other processing parameters are shown in Table 1. Four tensile samples were prepared for each joint according to ASTM standards E8M-04 [12]. Two samples of each condition were tested using the DIC technique with a 250 kN MTS machine. The remaining two tensile samples were tested using a 100 kN MTS tensile machine with a laser extensometer. All the tensile samples had a gage length of 25 mm and were tested at room temperature using a constant displacement rate of 2 mm/min. Scanning electron microscopy with a JOEL JSM840 was performed at 15 kV to analyze the fracture surface for some select samples.

DIC was carried out with an ARAMIS 3D optical deformation analysis system developed by GOM (Gesellschaft für Optische Messtechnik), Germany. The surface treatment for DIC consisted of applying a white color on the gage length of the sample, followed by spraying, with a refined airbrush, black speckles onto the white background. Two cameras were used to obtain the 3-D deformation of the samples. To build the 3-D information, the software correlates the images captured during tensile testing and records the deformation data at each stage.

Results and discussion

Table 1 shows the main laser processing parameters used in this study along with the failure locations of the tensile samples for each welding condition. It is noteworthy that the samples welded at a defocusing distance of -1 mm and welding speeds of 1.75 and 2.0 m/min were not fully penetrated. Thus these two samples were welded again from the opposite side (root) using the same processing parameters as the first weld.

Fig. 1 shows the effect of welding speed and defocusing distance on the global tensile properties obtained from the testing of four welded joints. The dashed lines in Fig. 1 show the associated mechanical property values for the BM. The yield stress and ultimate tensile stress remain almost constant for all the welding speeds and defocusing distances except for the sample that was welded at a welding speed of 0.75 m/min and a defocusing distance of -2 mm. The elongation at break is also the lowest for this sample. These global tensile properties that were obtained from both DIC and conventional tensile testing were found to be similar and thus confirm the reliability of the data.

Table 1 shows the failure locations and average joint efficiencies of all the tensile samples. Overall, the average joint efficiency is calculated as 100.16% in terms of the UTS and ranges from a minimum value of 96.79% to a maximum value of 100.94%. It was determined that porosity is the main reason for the tensile failure in the FZ for the joints welded at the lowest welding speed (0.75 m/min) and a defocusing distance of either -1 mm or -2 mm. This is due to the presence of a cluster of pores in the FZ, as observed from the fracture surface using scanning electron microscopy (Fig. 1b). At such a low welding speed of 0.75 m/min, the keyhole may collapse and lead to the formation of porosity. Table 1 reveals that both the porosity area and the percentage of the porosity area decrease with increasing welding speed for all the fully penetrated joints.

Table 1: Laser parameters, structural characteristics and failure locations

Welding speed (m/min)	Defocusing (mm)	Porosity area (mm^2)	Porosity area (%)	Max. underfill depth (mm)	Failure locations	Joint efficiency (%)
0.75	-1	0.295	1.36	0.22	4 FZ	100.56
1.0	-1	0.006	0.041	0.24	4 BM	100.94
1.5	-1	0.004	0.038	0.38	4 HAZ	99.72
1.75	-1	0.004 (*0.005)	0.044 (*0.055)	0.19	1 BM + 2 FZ + 1 HAZ	100.85
2.0	-1	0.115 (*0.06)	1.46 (*0.53)	0.07	4 BM	100.75
0.75	-2	0.155	0.64	0.2	4 FZ	96.79
1.0	-2	0.0725	0.468	0.29	3 HAZ + 1 BM	100.94
1.5	-2	0.0135	0.1365	0.33	4 HAZ	100.75

* Porosity values measured for a two-sided weld (used to correct the narrow root and lack of penetration)

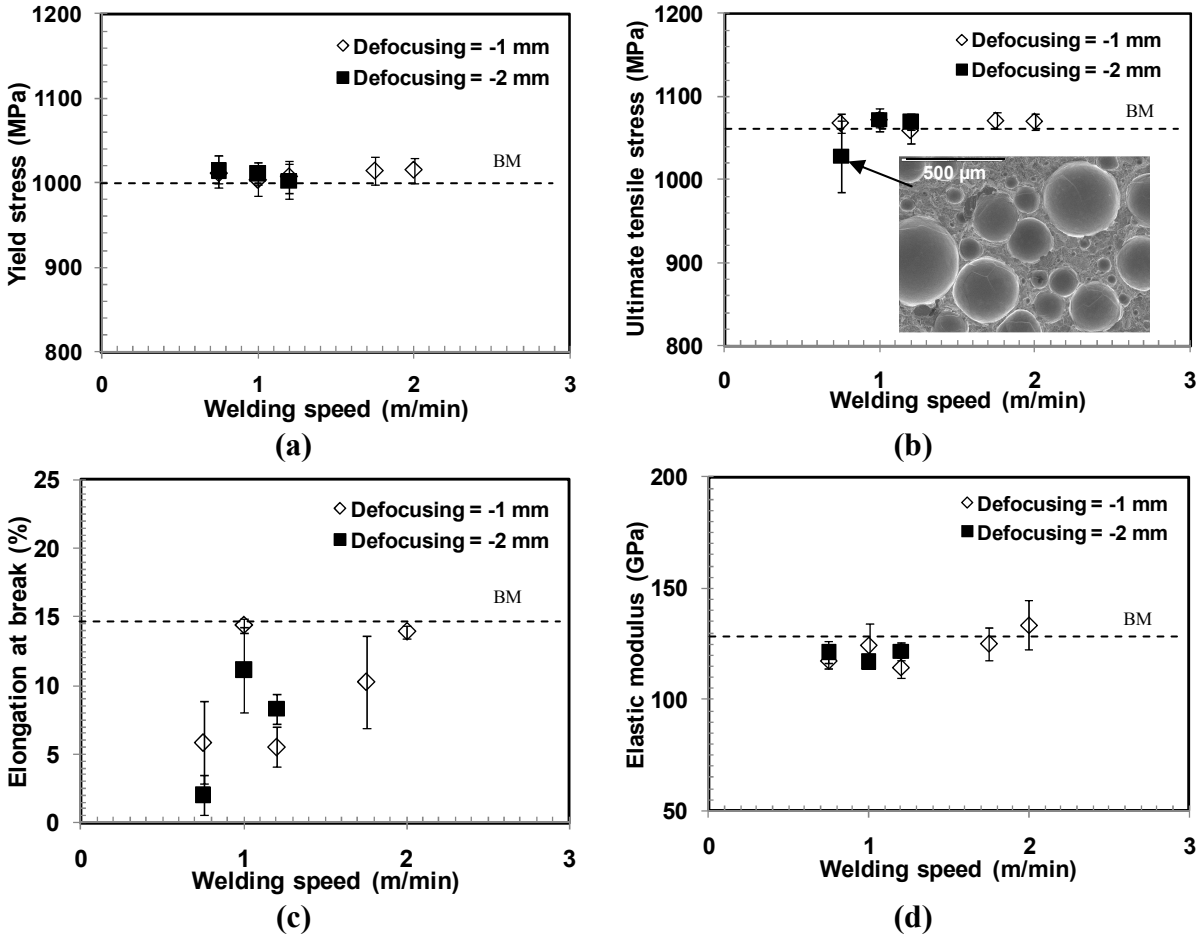

Fig. 1 Effect of welding speed on global tensile properties for 2 defocusing distances

The strain maps just before fracture (Fig. 2b), for the samples that failed in the FZ (i.e. 0.75 m/min), show maximum strains at the region of the underfill defects, which suggests that fracture initiated from the underfill defect and propagated through the weak FZ that contained a cluster of pores. The failure in the HAZ (Fig. 2c) is also due to the underfill defect. This sample was welded at an intermediate welding speed (~1.5 m/min) and has a maximum underfill depth, but extremely low porosity in the FZ, as shown in Table 1. As a consequence, the crack forms from the maximum underfill defect and propagates through the HAZ, since the FZ has a higher resistance due to the lower porosity. Failure may appear in the BM when both the FZ and the HAZ have fewer defects (underfill and porosity, respectively). Hence, it is clear that the tensile failures preferentially form from the underfill defect. The propagation of the crack depends on the amount of porosity in the FZ.

If the porosity area is high (≥ 0.15 mm^2), the crack is more likely to propagate through the FZ. Although the allowable maximum underfill depth is specified as 0.36 mm according to the AWS D17.1 [13] for 5.1-mm thickness, an underfill depth of 0.29 mm was found to be the maximum tolerance in this study. That is, at an underfill depth of 0.24 mm for the sample welded at a defocusing distance of -1 mm and a welding speed of 1.0 m/min, all four samples fail in the BM. On the other hand, an underfill depth of 0.33 mm, for the sample welded at a defocusing distance of -2 mm and a welding speed of 1.5 m/min, resulted in all four samples failing in the HAZ. Between these two values, an underfill depth of 0.29 mm, obtained for the sample welded at a defocusing distance of -2 mm and a welding speed of 1.0 m/min, resulted in three among four samples failing in the HAZ. If the underfill depth is high (≥ 0.29 mm), the crack propagates through the HAZ as long as the porosity area remains less than the threshold (i.e. 0.15 mm^2).

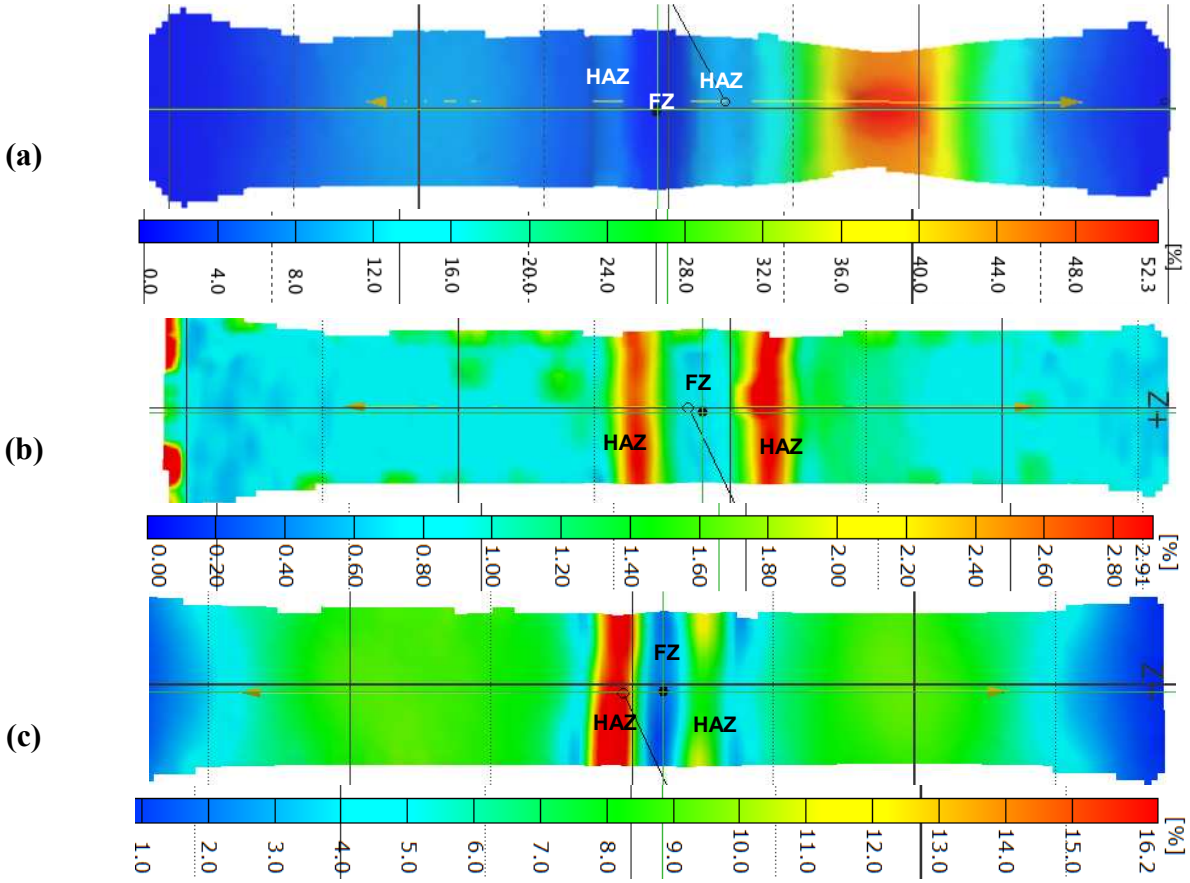

Fig. 2 Strain maps just before fracture. (a) failure in BM at defocusing -1 mm and 1.0 m/min, (b) failure in FZ at -2 mm and 0.75 m/min, and (c) failure in HAZ at -2 mm and 1.5 m/min

Fig. 3 shows the local tensile properties (extracted from the ARAMIS system) throughout the gage lengths of the samples joined at a welding speed of 1.0 m/min for the two defocusing distances just before fracture. Compared to the BM, the elastic modulus is higher in the FZ and lower in the HAZ. The yield stress is also slightly higher in the FZ and lower in the HAZ, as compared to the BM. The localized plastic strain was maximum in the fracture zone (BM) and almost no plastic deformation appears in the FZ, as shown in Fig. 3c. Although the fracture occured in the HAZ for the sample at a defocusing distance of -2 mm and a welding speed of 1.0 m/min, the local maximum plastic strain is located in the BM. Therefore, the fracture will not always occur at the position with the maximum plastic strain.

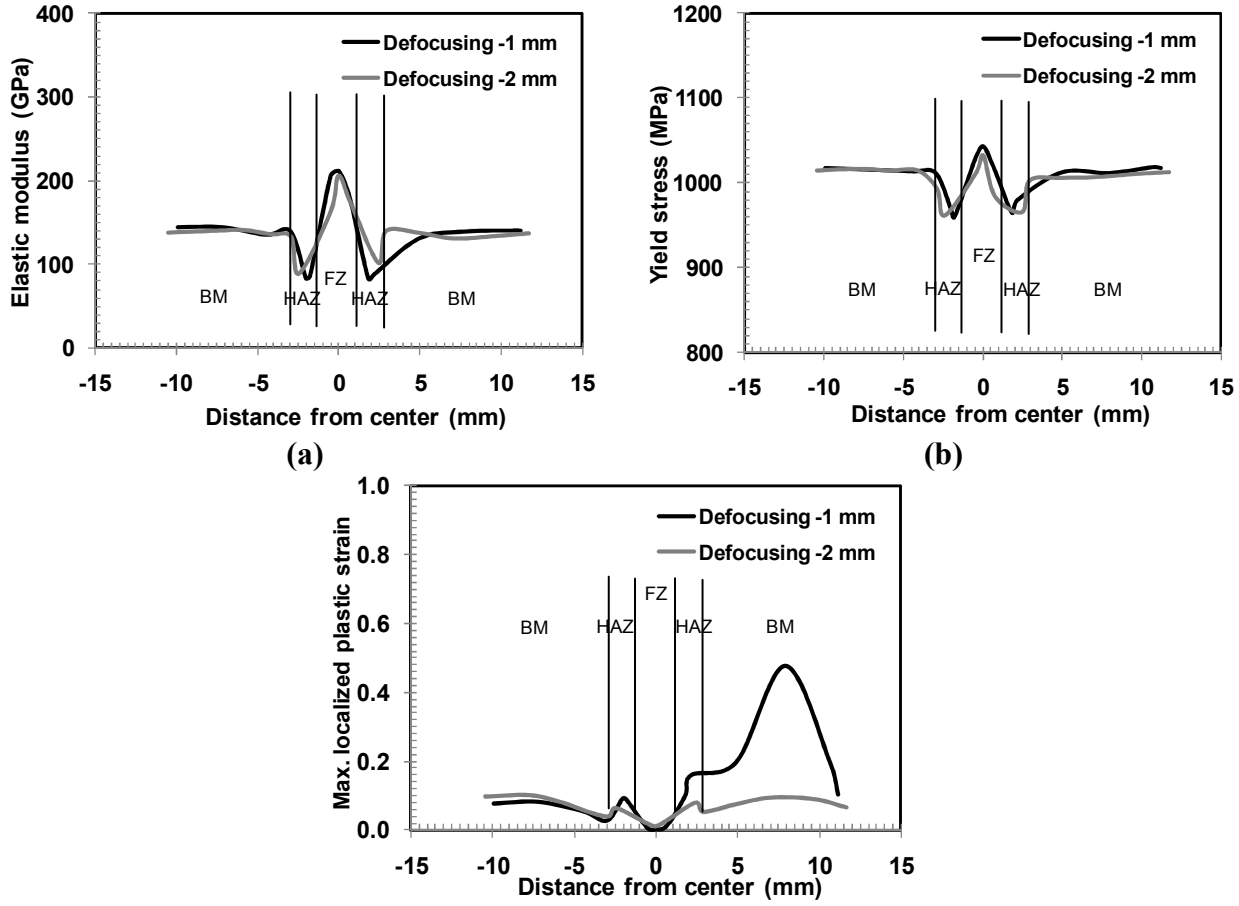

Fig. 3 Local tensile properties just before fracture at Defocusing -1 mm, 1.0 m/min and Defocusing -2 mm, 1.0 m/min

Fig. 4 shows the SEM fractographic images of the samples joined at a defocusing distance of -1 mm with a welding speed of 1.0 m/min and a defocusing distance of -2 mm with a welding speed of 0.75 m/min.

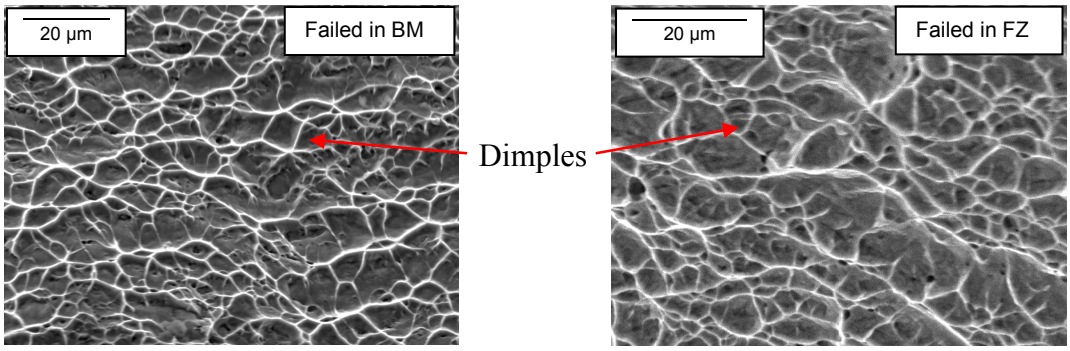

(a) Defocusing -1 mm, 1.0 m/min **(b) Defocusing -2 mm, 0.75 m/min**

Fig. 4 SEM fracture surfaces

The first sample failed in the BM (Fig. 4a) and the second one failed in the FZ (Fig. 4b). For the two samples, fractographic analysis revealed the presence of a dimpled structure on the fracture surfaces, indicating that micro-void coalescence is the mechanism for fracture regardless of whether ductile failure occurs in the BM (Fig. 4a) or FZ (Fig. 4b).

Conclusions

The 5.1-mm thick Ti-6Al-4V alloy sheets were welded autogenously using a 4 kW Nd: YAG laser at the following process parameters: laser power 4 kW, welding speed from 0.75 m/min to 2.0 m/min, and defocusing distances -1 mm or -2 mm. The following conclusions can be drawn:

1. The overall yield strength and elastic modulus remain relatively constant over the welding speeds and the two defocusing distances studied in this work. A similar tendency is obtained for the ultimate tensile strength, but these strength values can be compromised by the collapse of the instable keyhole that transpires at a welding speed lower than 1 m/min.
2. Compared with the base metal, a higher elastic modulus and yield stress are obtained in the fusion zone. In contrast, a lower elastic modulus and yield stress appear in the HAZ.
3. Tensile failure is mainly determined by the two main welding defects observed, i.e. underfill and porosity. Cracks usually form at the underfill defect if it is deeper than the threshold value of approximately 6% of the work-piece thickness. The cracks can then propagate along the fusion zone when the porosity level is high, or through the HAZ, if the fusion zone is strong due to a low porosity level. If both the underfill depth and porosity level are low, the welds appear to be stronger than the base metal, as failure usually appears in the base metal.

Acknowledgements

The authors would like to thank E. Poirier, X. Pelletier and D. Chiriac for their technical supports.

References

[1] X. Cao and M. Jahazi: Optics and Lasers in Engineering Vol. 47 (2009), p. 1231.
[2] X. Cao, G. Debaecker, E. Poirier, S. Marya, J. Cuddy, A. Birur and P. Wanjara: J. Laser Appl. Vol. 23 (2011), doi:10.2351/1.3554266.
[3] J. L. Barreda, F. Santamaría, X. Azpiroz, A. M. Irisarri and J. M. Varona: Vacuum Vol. 62 (2001), p. 143.
[4] X. Cao, G. Debaecker, M. Jahazi, S. Marya, J. Cuddy and A. Birur: Mater. Sci. Forum Vol. 638 (2010), p. 3655.
[5] M. J. Donachie, Titanium: A Technical Guide, ASM International, Materials Park, OH 1989.
[6] P. Wanjara, M. Brochu and M. Jahazi: Materials and Manufacturing Processes Vol. 21 (2006), p. 439.
[7] ASM Handbook, Welding, Brazing, and Soldering, Vol. 6, ASM International, Materials Park, OH 1993.
[8] J. Mazumder and W. Steen: Metall. Mater. Trans. A Vol. 13 (1982), p. 865.
[9] W. D. Lockwood and A. P. Reynolds: Mater. Sci. Eng. A Vol. 339 (2003), p. 35.
[10] B. Boyce, P. Reu and C. Robino: Metall. Mater. Trans. A Vol. 37 (2006), p. 2481.
[11] M.A. Sutton, W.J. Wolters, W.H. Peters, W.F. Ranson and S.R. McNeill: Image and Vision Computing Vol. 1 (1983), p. 133.
[12] ASTM, in E 8M-04, American Society for Testing and Materials, PA, USA 2004.
[13] AWS, in D17.1, American Welding Society, Ohio, USA 2001.